

# Microseismicity Recorded by a Fiberoptic Ocean-bottom PRM Installation Offshore Brazil

A.V. Goertz\* (PGS), J. Richardson (PGS), J. Faragher (PGS), C. Remington (Microseismic Inc.), P. Morton (Microseismic Inc.), P. Barros (Petrobras) & C. Theodoro (Petrobras)

## SUMMARY

---

A significant number of microseismic events were detected over 120 days of passive monitoring with a deepwater PRM pilot array offshore Brazil. The array is installed in 1240-1310m water depth and consists of over 700 four-component stations. Recording occurred during two consecutive two-month periods in between active seismic surveys. The passive monitoring detected distinct event swarms that are highly clustered in space and time. These events occur at an estimated depth of about 5 km with moment magnitudes ranging from 0.2 to 1.9. The seismicity occurs in a depth interval near a currently undeveloped deeper reservoir and is possibly of natural origin. The capture of such seismicity is valuable input for long-term risk assessment and development planning of the lower reservoir.

## **Introduction**

A significant aspect of the value proposition for permanent ocean bottom installations is the ability to continuously and passively record the ambient seismic wave field. Such data can be used for microseismic monitoring of the reservoir and overburden. Microseismic events from within or around a producing reservoir can be indicative of reservoir fluid pathways and sub-seismic reservoir compartmentalization (e.g., Maxwell & Urbancic, 2001), or stress changes and associated production-related deformations in the vicinity (e.g., Teanby et al., 2004, Zoback & Zinke, 2002). Continuous monitoring of seismicity can also help in assessing deformation-related risks to infrastructure over the life cycle of a field. The ambient seismic and acoustic noise at the ocean bottom can also be processed interferometrically for applications such as shallow hazard surveying (Dellinger et al., 2013).

Existing ocean-bottom PRM installations are predominantly in shallow water and have so far not been able to detect levels of microseismic activity in the vicinity of the reservoir that would allow a quantitative interpretation of the event cloud for reservoir characterization and risk assessment. Reasons include not only the high acoustic noise environment at the ocean bottom, especially in the North Sea (e.g., Olofsson, 2010), but also a lack of adequate processing methods that are scalable for typical installations with several thousands of channels. Microseismic recordings from an offshore oilfield environment exist, but predominantly from temporary borehole installations (Maxwell & Urbancic, 2001, de Meersman et al., 2009). Borehole seismic monitoring requires the availability of wellbores that are adequately located, reasonably quiet (preferably no producer or injector), and suitable for the permanent deployment of seismic equipment. A combination of the above at reasonable cost is a very rare occurrence. It would therefore be preferable if microseismic monitoring could also be achieved from the ocean bottom, where adequate coverage and aperture can be achieved at comparatively reasonable cost.

We present microseismic data from a deepwater installation offshore Brazil. The main goal of this limited-time passive recording was to provide proof of concept that microseismic monitoring is generally feasible with a deepwater ocean bottom PRM array. Through continuous recording over several months, we were able to detect highly clustered seismicity clouds at about 5 km depth in an area that contains a currently undeveloped oil reservoir. No seismicity was detected from the shallower, producing reservoir, indicating that the current reservoir is either producing without significant brittle deformation, or the recording period was too short to reliably detect seismicity at the currently achievable detection threshold. Nevertheless, despite the limited-time recording, a sufficient number of seismic events were recorded from the deeper, undeveloped reservoir to allow for a qualitative interpretation. This data not only proves the concept for microseismic recording in this installation, but also allows for some recommendations for recording and processing of ocean-bottom microseismic data.

### **The Jubarte deepwater PRM installation**

The fiber-optic deepwater pilot PRM installation over the Jubarte field in Brazil's Campos basin consists of 712 seismic recording stations along two cables, covering an area of about 9 km<sup>2</sup> (Figure 1). A subsea assembly merges these cables into an umbilical leading up to a FPSO, where the optical signals are demodulated and digitized. With water depths from 1250 to 1350 m, this was the world's deepest PRM when installed in late 2012. Each station consists of 4 channels, one pressure sensor, and three non-gimballed, orthogonally oriented acceleration sensors. The seismic acquisitions so far include a baseline and monitor active seismic survey (with a second monitor scheduled for late 2014), and two passive recording periods of 2 months duration each. Results from the 1<sup>st</sup> monitor active seismic survey are reported at this conference in Lecerf et al.. The radial vector components of the acceleration sensors are arbitrarily oriented upon deployment and their orientation angles need to be resolved firstly. We use the shots from the baseline active seismic survey which provide a highly redundant number of calibration points for this purpose.

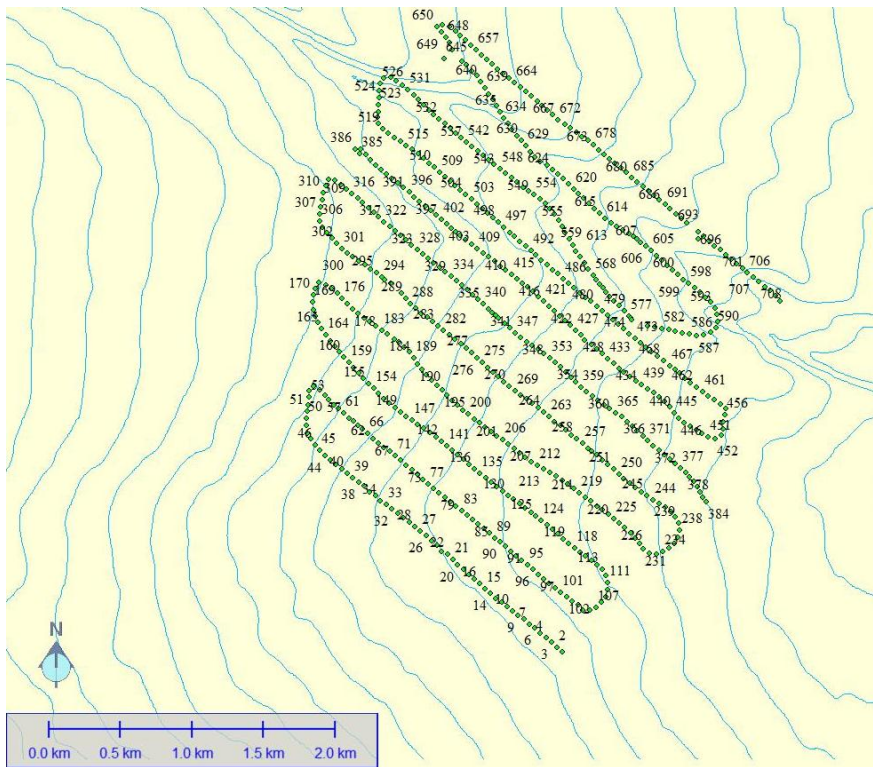


**Figure 1** Layout of the fiber optic ocean bottom cable (green) with 10 m bathymetry contours (blue).

Figure 2 shows an example microseismic event before (left) and after (right) rotation of the acceleration components. The direct P, its sea surface reflection, and the direct shear arrival can be clearly distinguished (blue arrows on the left side). After rotation, the first arrivals on the acceleration components line up, adding to a more coherent impression in the shot gather. Note how the P- and S energy separates into different components after rotation, highlighting the excellent vector fidelity of the sensors. After rotation, P-wave energy is concentrated on the vertical and hydrophone components, whereas significant shear wave energy is visible on the horizontal components.

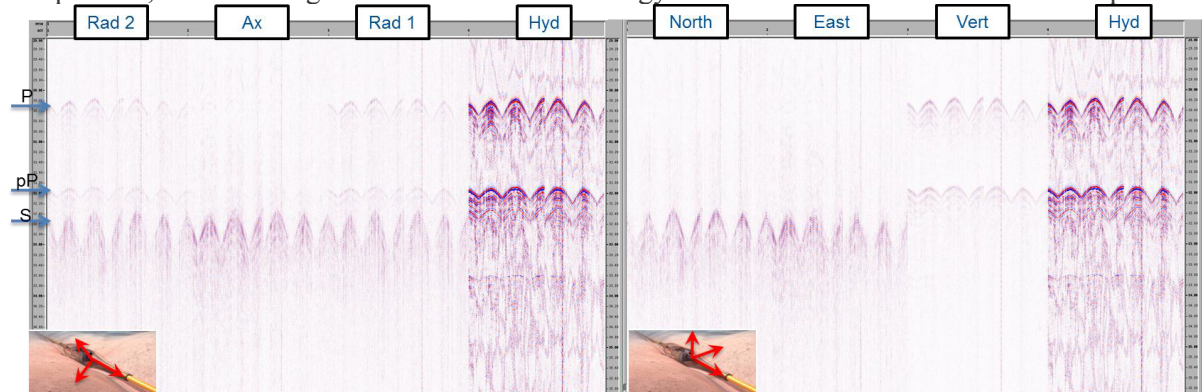


**Figure 2:** 4C shot gather of a microseismic event before (left) and after (right) rotation. P and S wave energy separates into different components after rotation. Data are filtered 5-70 Hz.

## Microseismic Results

The continuous data were processed with an automatic Kirchhoff-based depth imaging and coherency-driven event detection algorithm (Duncan & Eisner, 2010). Out of this process, we obtain, after careful QC, about 110 microseismic event locations for the 1<sup>st</sup> monitoring period (from June to August, 2013), and about 500 events for the 2<sup>nd</sup> monitoring period (March-May, 2014). All of these events are located in depths of 4500 to 5500 m, with events from the 1<sup>st</sup> period locating deeper and further to the south than events from the 2<sup>nd</sup> monitoring period. Apart from strong spatial clustering,

all events are also highly clustered in time and occurred during short time periods of less than a day each. Comparison with a regional conventional streamer seismic volume reveals that the location of the events and shape of the event cloud appears to be consistent with fault orientations discernible from the seismic volume. This is further corroborated by moment tensor inversions of selected events that exhibit a normal faulting mechanism consistent with the main structural trends in the 3D seismic at that depth. Figure 3 shows an example depth slice of the 3D seismic volume at 5000 m, together with the event clouds of both monitoring periods. The location of the monitoring array is outlined. The events are located in the lower portion of the sedimentary section near a depth interval where a deeper oil reservoir is located. The deeper reservoir was undeveloped in the area at the time of the occurrence of these events. The main target of the PRM array is a producing shallower reservoir from which no seismicity was detected.

Microseismic processing also included the determination of moment magnitudes of these events, ranging from +0.2 to +1.9. The detection threshold is lower for the second monitoring period than for the 1<sup>st</sup>. This has two main reasons. On the one hand, the events are located somewhat closer to the array for the 2<sup>nd</sup> period. On the other, and more importantly, the background noise level is significantly different between the two monitoring periods, with period 1 exhibiting a strongly elevated noise level compared to period 2. This included not only increased man-made noise from field activity, but also increased weather-related swell noise during the 1<sup>st</sup> period. The 1<sup>st</sup> period was acquired during the southern winter (June-August) with correspondingly higher sea states than the 2<sup>nd</sup> passive acquisition which was acquired towards the end of the southern summer (March-May). Figure 4

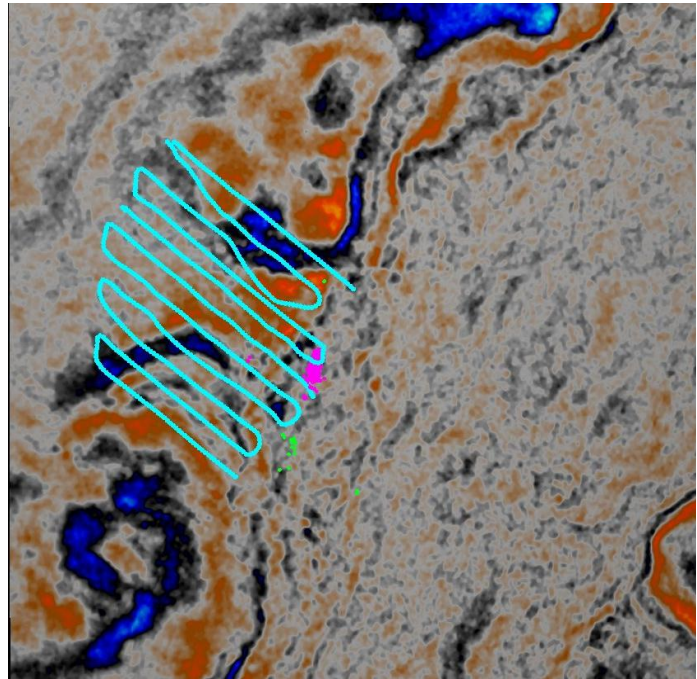


**Figure 3:** Depth slice from regional 3D seismic at 5000 m. Dots denote events from both monitoring periods (green 1<sup>st</sup>, and purple 2<sup>nd</sup>). Location of the PRM array is outlined in light blue.

(left) shows a magnitude vs. distance plot, with distance measured from the centre of the array. Note the lower detection threshold of about +0.2 for the second monitoring period. So far only P-wave data on the hydrophone component was used for processing. We expect that the detection threshold can be further lowered when all four components and shear wave information are used in the processing.

Accurate magnitudes are important for long-term risk assessment. The Gutenberg-Richter law prescribes that the distribution of event magnitude follows a power law of the form  $N = 10^{a-bM}$ , where  $M$  is magnitude,  $N$  is the number of events with that magnitude, and  $a$  and  $b$  are dimensionless constants. If we know the  $b$ -value, and the number of events that occurred in a certain time period, we can extrapolate if significantly larger events, potentially causing damage to infrastructure, could potentially occur over the projected life time of the field. While two rather arbitrarily chosen 2-month periods of recording are certainly not enough for an authoritative long-term prognosis, we note that enough seismicity was captured to actually measure a  $b$ -value and establish a preliminary Gutenberg-Richter statistic (Figure 4, right). We obtain a  $b$ -value of 2.4, which is relatively high in comparison.

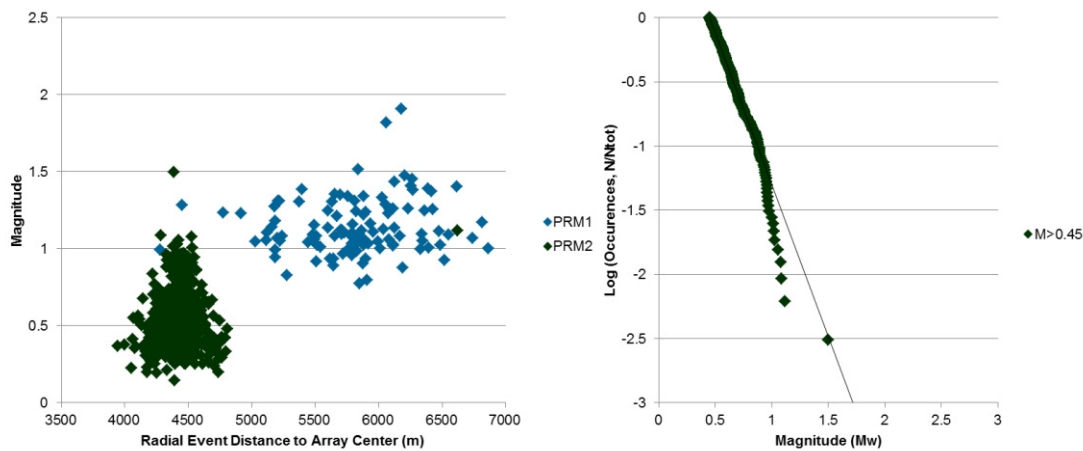


**Figure 4:** Left: Magnitude vs. distance plot for both monitoring periods (blue: 1<sup>st</sup>, green, 2<sup>nd</sup>). Right: Frequency-magnitude statistic (Gutenberg-Richter plot) for the 500 events of the 2<sup>nd</sup> period.

## Conclusions

Passive recording with the Jubarte deepwater PRM array captured microseismicity from depths in excess of 4500 m, in an interval that contains a currently undeveloped deeper oil reservoir, unconnected to shallower production. The shape of event clouds and inverted fault plane solutions are consistent with extensional-style structural features observable in 3D seismic. The lack of correlation with field infrastructure and the magnitude of the events point to the seismicity being of natural origin. High b-values could indicate that the seismicity is still fluid-driven, albeit it appears unlikely to be related to current oil production. The detection of this level of seismicity is important information for risk assessment relating to the development of the lower reservoir. Longer passive acquisitions before, and during field development should be part of the de-risking strategy. No seismicity was detected from the shallower reservoir. However, a longer recording period and a lower detection threshold through 3C processing may also reveal production-induced seismicity from the shallower reservoir. We hope that some of the microseismic lessons learned from this deepwater PRM installation could be extrapolated to shallower water depth installations.

## Acknowledgements

We thank Petrobras for permission to publish the results. Ed Hodges helped with some displays.

## References

- Dellinger, J., S. de Ridder, A. Mordret, N. Shapiro, O. Barkved, J. Yu, 2013, Progress towards a Passive Shallow-subsurface Continuous-monitoring System at Valhall Using the LoFS Array, 75th EAGE Conference & Exhibition, DOI: 10.3997/2214-4609.20130194.
- DeMeersman, K., J. Kendall, and M. van der Baan, 2009, The 1998 Valhall microseismic data set: An integrated study of sources, seismic multiplets, and S-wave splitting: *Geophysics* **74**,5,B183-B195.
- Duncan, P. M., and L. Eisner, 2010, Reservoir characterization using surface microseismic monitoring: *Geophysics*, **75**, no. 5, A139–A146 <http://dx.doi.org/10.1190/1.3467760>.
- Maxwell, S. C., and T. Urbancic, 2001, The role of passive microseismic Monitoring in the instrumented oil field: *The Leading Edge*, **20**, 636–639.
- Olofsson, B., 2010, Marine ambient seismic noise in the frequency range 1-10 Hz: *The Leading Edge*, **29**, 4, 418–435, doi:10.1190/1.3378306.
- Teanby, N., J.-M. Kendall, R. Jones, and O. Barkved, 2004, Stress-induced temporal variations in seismic anisotropy observed in microseismic data: *Geophysical Journal International*, **156**,459–466.
- Zoback, M. D., and C. Zinke, 2002, Production-induced normal faulting in the Valhall and Ekofisk oil fields: *Pure and Applied Geophysics*, **159**, No.1, 403–420.